PHYSICAL REVIEW C VOLUME 15, NUMBER 4 APRIL 1977

Calculation of (n,p) scattering observables with a separable R matrix between 20 and 140 MeV†

F. Pauss and H. F. K. Zingl
Institute for Theoretical Physics, University of Graz, Graz, Austria
(Received 11 February 1976)

We calculated the differential cross section and polarization (I_0, p_y, C_{yy}, and K_z^x) for (n,p) scattering at energies between 20 and 140 MeV with a separable potential model. It is shown that (a) the potentials fitted to the results of an unconstrained phase shift analysis cannot reproduce the experimental data and (b) the mixing parameter ϵ_1 is most probably positive at all energies and a smoothly varying function of the energy. More polarization experiments are needed to settle these questions unambiguously.

[NUCLEAR REACTIONS (n,p) scattering observables, 20–140 MeV calculated with separable R matrix.]

I. INTRODUCTION

The rapid progress in the phenomenology of the two-nucleon system achieved in the last two decades was summarized by several authors[1-3] who pointed out also the fundamental difficulties of the theory. Recently many suggestions were made to obtain a more precise representation of the experimental data even at the cost of replacing the simpler forms of the potential by introducing heavier meson exchange[4,5] and more complicated separable potentials.[6-12] Fitting the free parameters of these phenomenological potentials in the usual way[13] particular problems arise in connection with the large uncertainty in the values of the mixing parameter ϵ_1 at low energies[14] for the important (n,p) channel $^3S_1$-$^3D_1$. In addition to this, negative ϵ_1 values obtained in previous phase shift analyses for energies below 80 MeV cannot be ruled out.[15]

A direct correlation between the experimental data and a given potential model may give, however, more information on the above problems. Therefore a direct calculation of the (n,p) observables, e.g., I_0, p_y, C_{yy}, and K_z^x, from the given potential becomes increasingly important.[16] The main objective of the present paper is to study the above correlations with a particular emphasis to the energy dependence of the ϵ_1 phase at low energies and to suggest measurements to remove the ambiguities in the determination of the ϵ_1 values.

The theoretical foundation of the method used was elaborated by Stapp, Ypsilantis, and Metropolis[17] and refined calculations of the experimental observables were carried out, e.g., by Binstock and Bryan.[16] Our analysis differs from the previous ones essentially by using separable potentials in the calculations. Since we intend to show the changes in the scattering observables by varying the important $^3S_1$-$^3D_1$ channel we must choose for our calculations a standard potential which includes all partial waves except the $^3S_1$, ϵ_1, and $^3D_1$ waves. The basis for the selection of this potential was a discussion of the characteristic properties of the separable potentials given in a paper by Plessas *et al.*[18] In detail we have used for $^1S_0$, $^1D_2$, and $^3D_3$ the Graz potential,[8] and for $^1P_1$, $^3P_0$ (Set B), $^3P_1$, $^3P_2$, and $^3D_2$ the Doleschall[6] parametrization of these partial waves.

We studied the energy dependence of the (n,p) observables only between 20 and 140 MeV where the ambiguity in the $I=0$ phases is rather large, particularly in the 25–95 MeV range.[14] Therefore we considered in our calculations only partial waves with $L \leq 2$ for the standard potential. For the coupled $^3S_1$-$^3D_1$ channel we used the parametrizations given in Refs. 6–12. It is necessary to emphasize that we are not only varying the ϵ_1 phase[19] but carrying out the calculations with different partial wave potentials for the ^3S-^3D channel in order to study the influence of the whole coupled channel on the experimental observables.

Finally we also calculated the above cited observables (for a systematic picture see Appendix I) with a local potential model[20] and with the experimental phases given by Seamon *et al.*[21] and MacGregor *et al.*,[14] to see how well a separable potential model predicts observables compared with a local one and to experimental phases.

II. R MATRIX AND PHASE SHIFTS

We denote the spin wave function for the initial and final particles by χ_i and χ_f, respectively, and the relative momenta in the c.m. system by $\vec{k}_i$ and $\vec{k}_f$. Then the total final wave function is

$$\psi_f = \frac{1}{(2\pi)^{3/2}} e^{i\vec{k}_i\cdot\vec{r}}|\chi_i\rangle + \frac{1}{(2\pi)^{3/2}} \frac{e^{ik_f r}}{r} f(\vec{k}_f, \vec{k}_i) , \quad (1)$$

$$f(\vec{k}_f, \vec{k}_i) = M(\vec{k}_f, \vec{k}_i)|\chi_i\rangle , \quad (2)$$

where M is the spin scattering amplitude operating on the initial spin state and which is related to the usual scattering matrix[22,23]

$$M(\theta,\phi) = \frac{2\pi}{ik}\sum_{L,L'} \langle \theta_f\phi_f|S^J_{L'L} - \delta_{L'L}|\theta_i\phi_i\rangle \quad (3)$$

(θ and ϕ the c.m. angles). Performing a partial wave expansion this can be cast into the following form

$$\langle S'm_{s'}|M(\theta,\phi)|Sm_s\rangle = \frac{2\pi}{ik}\sum_L \sum_{J=|L-S|}^{|L+S|} \sum_{L'=|J-S|}^{|J+S|} \left(\frac{2L+1}{4\pi}\right)^{1/2} Y_{L'}^{m_s-m_{s'}}(\theta,\phi) C_{L'S}(Jm_s; m_s - m_{s'}, m_{s'})$$
$$\times C_{LS}(Jm_{s'}; 0m_s)\langle L'SJm_s|S_{L'L} - \delta_{L'L}|LSJm_s\rangle , \quad (4)$$

where C_{LS} are the Clebsch-Gordan coefficients,[24] m_s the z component of the spin s, and the quantization axis has been chosen along the direction of motion of the incoming particle. Let us define a set of new matrix elements α

$$\begin{aligned}
&\langle L0Lm_j|S_L - 1|L0Lm_j\rangle = \alpha_L, \quad S=0, L+J ,\\
&\langle L1Jm_j|S_{L'L} - 1|L1Jm_j\rangle = \alpha_{LJ}, \quad S=1, L'=L ,\\
&\langle J\pm1, 1Jm_j|S_{L'L} - \delta_{L'L}|J\mp1, 1Jm_j\rangle = \alpha^J, \quad S=1, L=J\pm1, L'=J\mp1 .
\end{aligned} \quad (5)$$

Following the commonly used notation $\langle 00|M|00\rangle = M_{ss}$ and $\langle 1m_{s'}|M|1m_s\rangle = M_{m_{s'}m_s}$ we obtain from Eq. (4) the explicit formulas for the various M matrix elements

$$M_{ss} = \frac{1}{ik}\sum_L P_L(\cos\theta)\tfrac{1}{2}(2L+1)\alpha_L , \quad (6)$$

$$M_{m_{s'},m_s} = \frac{2\pi}{ik}\sum_L \Bigg\{ \sum_{J=|L-1|}^{|L+1|} \left(\frac{2L+1}{4\pi}\right)^{1/2} C_{L1}(Jm_s; m_s - m'_s m_s) C_{L1}(Jm_{s'}; 0m_s)\alpha_{LJ}$$
$$- \sum_{J=L\pm1} \left(\frac{2L'+1}{4\pi}\right)^{1/2} C_{L'1}(Jm_{s'}; m_s - m_{s'} m_s) C_{L1}(Jm_{s'}; 0m_s)\alpha^L \Bigg\} Y_L^{m_s-m_{s'}}(\theta,\phi) . \quad (7)$$

The numerical calculation becomes simpler if we use the real R matrix instead of the complex T matrix which is connected with the R matrix by the Heitler equation.[23] Finally we obtain for the singlet case, $S=0, L=L'=J$:

$$\alpha_L = -\frac{2\pi i\rho_E R_L}{1 + i\pi\rho_E R_L} \quad (8)$$

with

$$\rho_E = \frac{k\mu}{\hbar^2}, \quad \mu = \frac{m_1 m_2}{m_1 + m_2}$$

and for the triplet case, $S=1, L=L'$:

$$\alpha_{LL} = -\frac{2\pi i\rho_E R_{LL}}{1 + i\pi\rho_E R_{LL}} ; \quad (9)$$

$S=1, \quad L=J-1=L_<,$

$L'=J-1=L_<,$

$L_{\ll} \equiv L_< L_<:$

$$\alpha_{\ll} = -\frac{2\pi i\rho_E}{D}[R_{\ll} + i\pi\rho_E(R_{\ll}R_{\gg} - R_{<>}^2)] ; \quad (10)$$

$S=1, \quad L=J+1=L_>,$

$L'=J+1=L_>,$

$L_{\gg} \equiv L_> L_>:$

$$\alpha_{\gg} = -\frac{2\pi i\rho_E}{D}[R_{\gg} + i\pi\rho_E(R_{\ll}R_{\gg} - R_{<>}^2)] ; \quad (11)$$

$S=1, \quad L=J-1=L_<,$

$L'=J+1=L_>,$

$L_{<>} \equiv L_< L_>:$

$$\alpha_{<>} = -\frac{2\pi i\rho_E}{D}R_{<>} \quad (12)$$

with

$$D = (1 + i\pi\rho_E R_{\ll})(1 + i\pi\rho_E R_{\gg}) + \pi^2\rho_E^2 R_{<>}^2 . \quad (13)$$

With the formulas given in Appendix II we are now able to calculate the observables for a given separable potential. The results of this calculation are compared with the values calculated directly from phase shifts using the following relations[17]

$$\alpha_{\ll} = \cos 2\bar{\epsilon}_J\, e^{2i\bar{\delta}_{L<}} - 1\ ,$$
$$\alpha_{\gg} = \cos 2\bar{\epsilon}_J\, e^{2i\bar{\delta}_{L>}} - 1\ , \qquad (14)$$
$$\alpha_{<>} = i \sin 2\bar{\epsilon}_j\, e^{i(\bar{\delta}_{L>} + \bar{\delta}_{L<})}$$

($\bar{\epsilon}$, $\bar{\delta}$ the usual bar phase shifts). The above comparison was carried out with the same experimental data which were used by Breit[21] and MacGregor[14] in their phase shift analysis.

III. RESULTS AND DISCUSSION

One can study all the curves in Figs. 1 to 8 in order to see the influence of different ^3S-^3D parametrizations (i.e., to determine which of the neutron-proton observables is most sensitive to ϵ_1). A comparison of the experimentally determined observables with the theoretically predicted ones showed that some of these quantities (especially the spin-transfer coefficients) are rather insensitive to ϵ_1 (see Fig. 9) in the whole energy

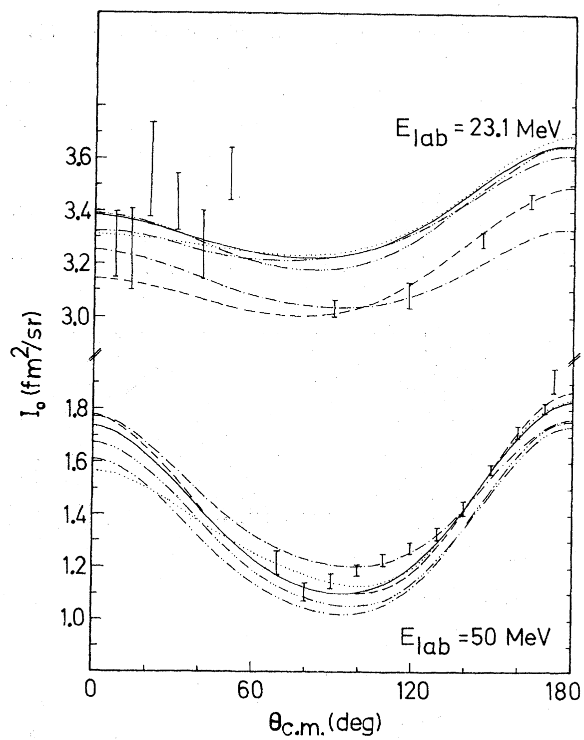

FIG. 1. Neutron-proton differential cross section I_0 at $E_{1ab} = 23.1$ and 50 MeV for the potentials Doleschall 3T4 (—••—), Doleschall *T4D* (—•••—), Doleschall *T4M* (•••), Reid (—•—) as well as computed with the phenomenological phase shifts of MacGregor *et al.* (——) and Breit *et al.* (---). In Figs. 1, 3, and 5 the calculations for Reid (—•—) and Breit (---) were done at 24 MeV instead of 23.1 MeV. Experimental values are taken from Scanlon *et al.* (Ref. 28) (data at $E_{1ab} = 22.5$ MeV), Rothenberg (Ref. 29) (data at $E_{1ab} = 24$ MeV), and Montgomery *et al.* (Ref. 30) (data at $E_{1ab} = 50$ MeV).

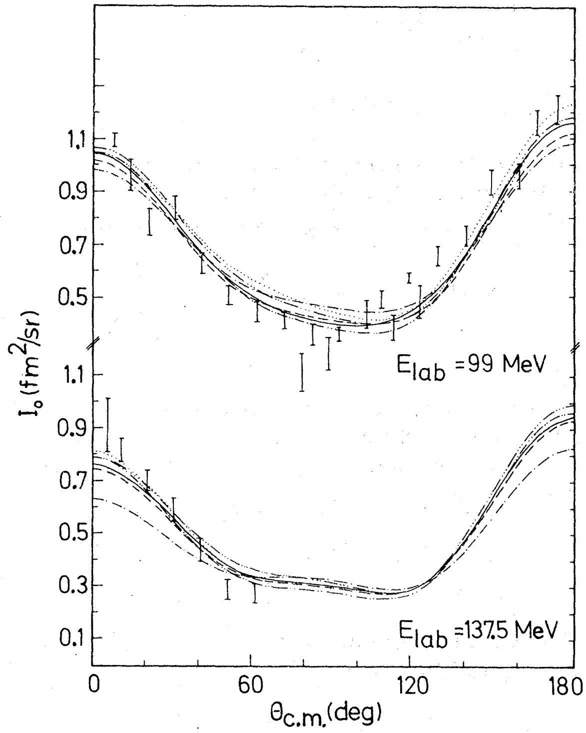

FIG. 2. Neutron-proton differential cross section I_0 at $E_{1ab} = 99$ and 137.5 MeV. Description of curves as in Fig. 1. Experimental data are taken from Wilson (Ref. 31).

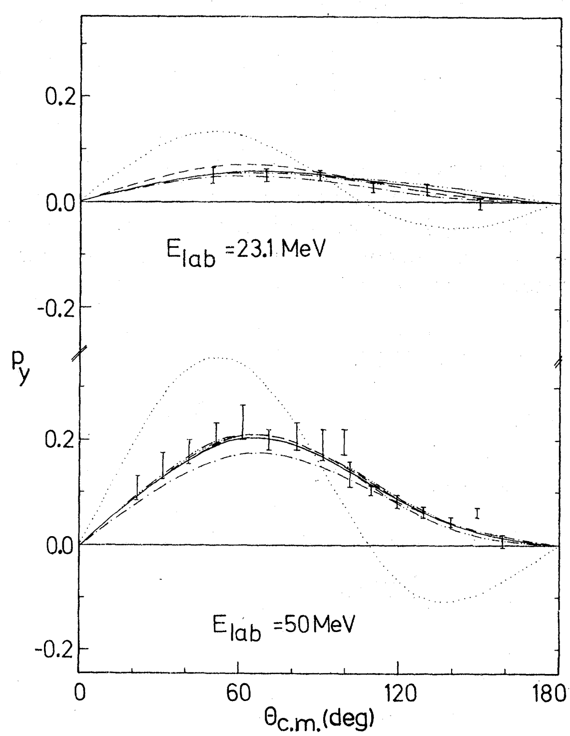

FIG. 3. Neutron-proton polarization p_y at $E_{1ab} = 23.1$ and 50 MeV. Description of curves as in Fig. 1. Experimental data are taken from Perkins *et al.* (Ref. 32) and Langsford *et al.* (Ref. 33).

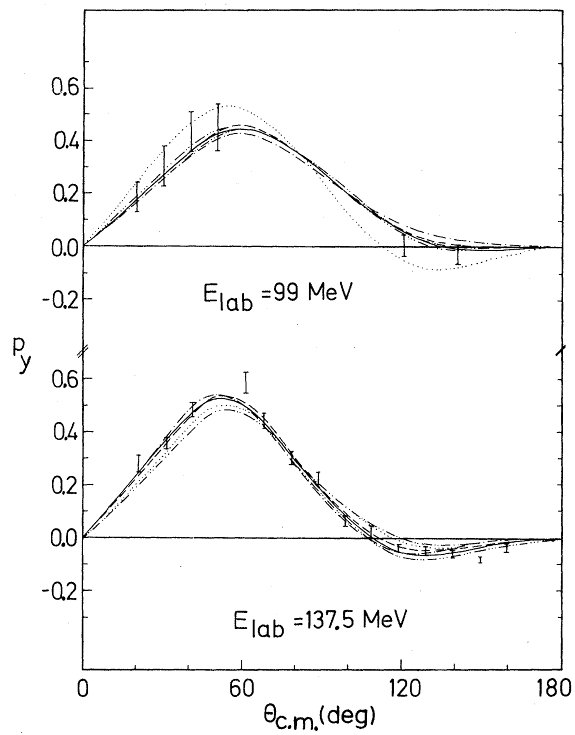

FIG. 4. Neutron-proton polarization p_y at $E_{1ab}=99$ and 137.5 MeV. Description of curves as in Fig. 1. Experimental data are taken from Wilson (Ref. 31, pp. 215 and 217).

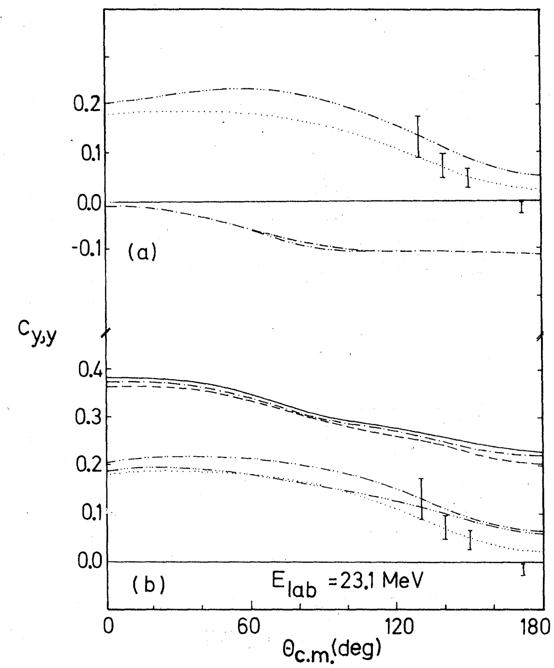

FIG. 6. (a) Neutron-proton spin correlation parameter $C_{y,y}$ at $E_{1ab}=23.1$ MeV for the potentials Mongan II (—•—•), Mongan IV (—••—), and Tabakin (—•••—); (b) for the potentials Graz preliminary (——), Graz I (---), Kahana b (—•—), Kahana a (—••—), and Hamman (—•••—) as well as MacGregor *et al.* (•••). Experimental data as in Fig. 5.

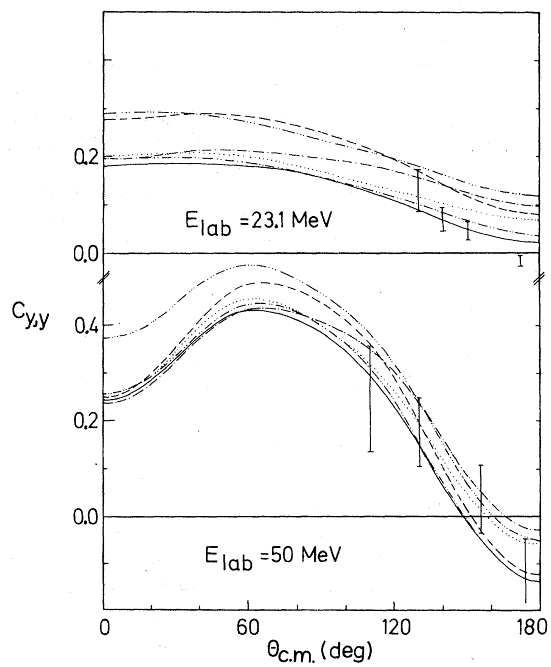

FIG. 5. Neutron-proton spin correlation parameter $C_{y,y}$ at $E_{1ab}=23.1$ and 50 MeV. Description of curves as in Fig. 1. Experimental data are taken from Simmons (Ref. 26) and Johnsen *et al.* (Ref. 27).

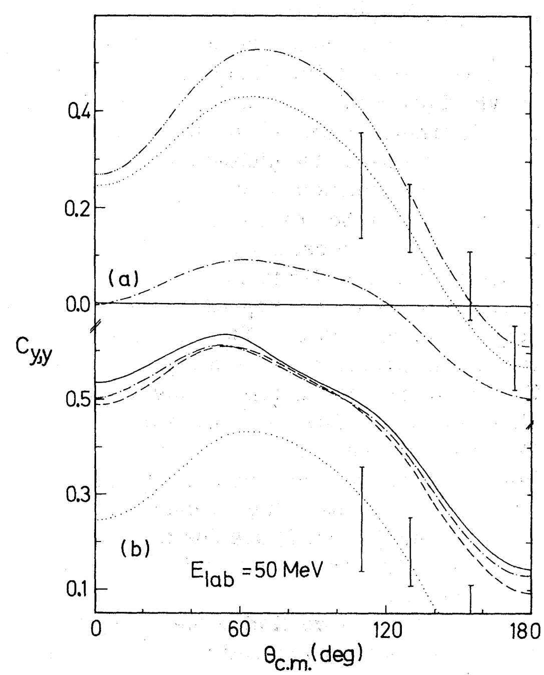

FIG. 7. (a), (b) Neutron-proton spin correlation parameter $C_{y,y}$ at $E_{1ab}=50$ MeV. Description of curves as in Figs. 6(a) and 6(b) and experimental data as in Fig. 5.

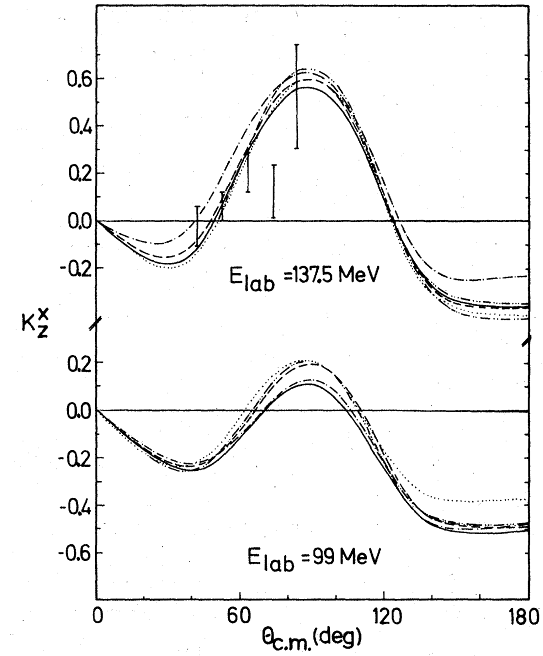

FIG. 8. Neutron-proton spin transfer coefficient K_z^x for $E_{lab} = 99$ and 137.5 MeV. Description of curves as in Fig. 1. Experimental data are taken from Hoffmann *et al.* (Ref. 34).

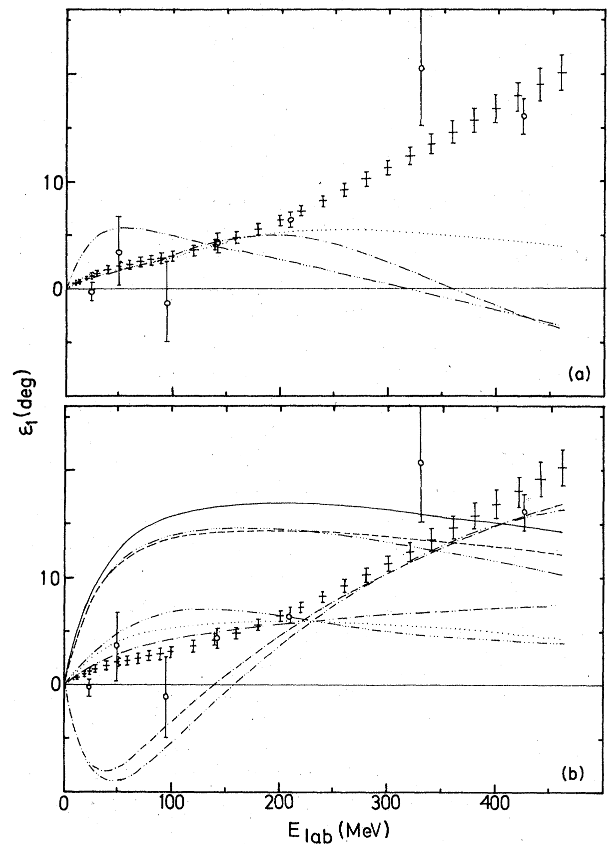

FIG. 9. (a) Mixing parameter ϵ_1 of the Doleschall potentials *T4M* (•••), *T4D* (—•••—), and 3*T4* (—••—). Dots and crosses mark the phenomenological phase shifts and their errors resulting from the energy-dependent phase shift analysis (constrained solution) and circles the corresponding quantities resulting from the energy-independent phase shift analysis of MacGregor *et al.* (Ref. 14). (b) Mixing parameter ϵ_1 of the potentials Graz I (——), Graz preliminary (---), Mongan II (—•—•), Mongan IV (—••—), Tabakin (—•••—), Kahana b (—•••••—), Kahana a (•••), and Hamman (—•—•). Description of experiment as in (a).

range considered.[25] Our results are in a good agreement with the results obtained by Binstock and Bryan[16] at 50 MeV.

Figures 1 and 2 show the behavior of the differential cross section I_0 calculated with our standard potential and using the different Doleschall parametrizations[6,7] for the coupled channel ${}^3S_1$-${}^3D_1$. We have also plotted the results obtained from the phenomenological local Reid soft-core potential,[20] and the results calculated by us directly from the latest Livermore[14] and Yale[21] phase shifts, in order to check also how well the experimental data are reproduced by the so-called "experimental" phases. The influence of the mixing parameter ϵ_1 on the differential cross section can be neglected; this is most clearly demonstrated by comparing the results of the Doleschall *T4D* and *T4M* parametrization. The slight deviations between the experimental data and the theoretical calculations at higher energies ($E_{lab} = 99$ and 137.5 MeV, Fig. 2) are due to the fact that we have restricted our calculations to $L \leq 2$ as shown in Ref. 18.

In Figs. 3 and 4 we plotted the calculated angular dependence of the polarization p_y with the experimental data. One can see easily that the curve obtained from the Doleschall *T4M* potential deviated significantly from the other curves. This is due to the fact that this parametrization cannot reproduce a reasonable ${}^3D_1$ phase shift. All other p_y curves are in a good agreement with each other and with the experimental data. According to this p_y is not sensitive to variations in ϵ_1.

Figures 5 to 7 show the calculated angular dependence of the spin correlation observable $C_{y,y}$ with the experimental data. From these curves more information can be obtained on the correlations between observables and the ϵ_1 phase. One can see from Fig. 5 that the results for the Doleschall *T4M* potential (good ${}^3S_1$, good ϵ_1, bad ${}^3D_1$) are in good agreement with the experimental values and the *T4D* potential (good ${}^3S_1$, bad ϵ_1, good ${}^3D_1$) yield to high values for $C_{y,y}$. In Figs. 6(a) and

7(a) the effect of negative ϵ_1 values can be studied with the Mongan potential which leads to unacceptable results for this observable. It can be shown, however, that too large positive ϵ_1 values, e.g., the Graz potential, also cannot reproduce the experimental values [Figs. 6(b) and 7(b)]. This shows a strong correlation between the ϵ_1 phase and the observable $C_{y,y}$ in agreement with the results of Binstock and Bryan,[16] Simmons,[26] and Johnsen *et al.*[27] Among the other polarization observables only K_z^x shows a slight sensitivity to ϵ_1 but only for energies beyond 137.5 MeV (Fig. 8).

Thus we conclude from our investigation of the correlations between observables and the mixing parameter ϵ_1 in the 20 to 140 MeV range that negative values for the ϵ_1 phase (e.g., the Mongan potential) do not lead to results in agreement with experimental data. From Figs. 6 and 7 it is easy to see that too large ϵ_1 values predict too large values for $C_{y,y}$ and too small ϵ_1 values (e.g., negative) predict too small $C_{y,y}$ values. Negative ϵ_1 values should be ruled out; ϵ_1 is most probably positive at all energies and a smoothly varying function of the energy. For more definite statements further refined measurements, e.g., of $C_{y,y}$ over the whole angular distribution and of energies up to 50 MeV, would be very important and from the theoretical point of view extremely desired. These measurements should make it possible to remove the ambiguities in the determination of the ϵ_1 values.

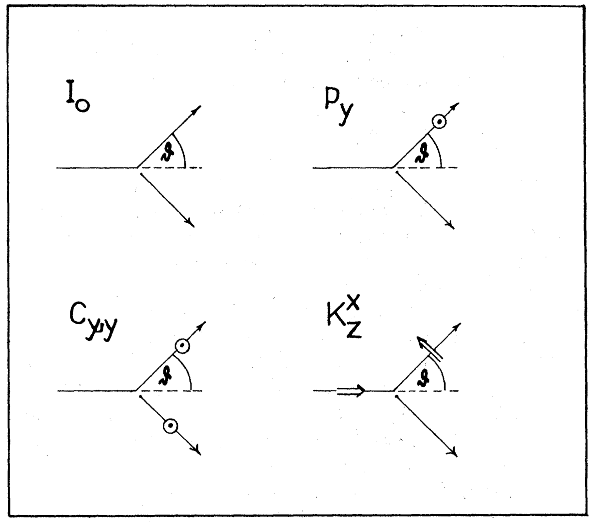

FIG. 10. Nucleon-nucleon observables; θ is the laboratory scattering angle; a circle with a center dot corresponds to spin normal to the scattering plane and out of the paper; an arrow with a wide shaft depicts spin lying in the scattering plane.

ACKNOWLEDGMENTS

We thank Dr. P. Doleschall for enlightening discussions and Mag. L. Mathelitsch for assistance with the computer program. We also wish to thank Professor E. Fenyves for helpful discussions and many valuable comments. The numerical calculations were performed at the UNIVAC 494 of the "Rechenzentrum Graz."

APPENDIX I

Systematic pictures of nucleon-nucleon observables calculated in this paper are given in Fig. 10. A complete listing of various observables can be found in the article of Binstock and Bryan (Ref. 16).

APPENDIX II

Observables in terms of M matrix elements:

$$I_0=\tfrac{1}{2}|M_{11}|^2+\tfrac{1}{4}|M_{00}|^2+\tfrac{1}{4}|M_{ss}|^2+\tfrac{1}{2}|M_{10}|^2+\tfrac{1}{2}|M_{01}|^2+\tfrac{1}{2}|M_{1-1}|^2,$$

$$I_0p_y=\tfrac{1}{4}\sqrt{2}\,\mathrm{Re}[i(M_{10}-M_{01})(M_{11}-M_{1-1}+M_{00})^*],$$

$$I_0(1-C_{y,y})=\tfrac{1}{2}(|M_{ss}|^2+|M_{11}+M_{1-1}|^2),$$

$$I_0K_z^x=-\tfrac{1}{2}\sin\tfrac{1}{2}\theta\,\mathrm{Re}\left\{\left[M_{00}+(\cos\theta+1)\frac{\sqrt{2}M_{10}}{\sin\theta}\right](M_{11}+M_{1-1}+M_{ss})^*-\left(\frac{\sqrt{2}}{\sin\theta}M_{10}+\frac{\sqrt{2}}{\sin\theta}M_{01}\right)(M_{11}+M_{1-1})^*\right\}.$$

†Supported by Fonds zur Förderung der wissenschaftlichen Forschung.

[1]M. J. Moravcsik, Rep. Prog. Phys. 35, 587 (1972).
[2]G. E. Brown and A. J. Jackson, *The Nucleon-Nucleon Interaction* (North-Holland, Amsterdam, 1976).
[3]J. S. Levinger, in *Springer Tracts in Modern Physics* (Springer Verlag, Berlin, 1974), Vol. 71, p. 88.
[4]K. Holinde and R. Machleidt, Nucl. Phys. A247, 495

(1975).

[5]R. Vinh Mau, in *Few Body Dynamics*, Proceedings of the Seventh International Conference on Few Body Problems in Nuclear and Particle Physics, Delhi, 1976, edited by A. N. Mitra, I. Šlaus, V. S. Bhasin, and V. K. Gupta (North-Holland, Amsterdam, 1976), p. 472.

[6]P. Doleschall, Nucl. Phys. A220, 491 (1974).

[7]P. Doleschall (private communication). We thank Dr. P. Doleschall for the new potential parameters for the 3*T*4 parametrization prior to publication. The properties are given in Ref. 18.

[8]L. Črepinšek, C. B. Lang, H. Oberhummer, W. Plessas, and H. F. K. Zingl, Acta Phys. Aust. 42, 139 (1975); and in *Few Body Problems in Nuclear and Particle Physics*, Proceedings of the Laval Conference, Quebec 1974, edited by R. J. Slobodrian, B. Cujec, and K. Ramavataram (Les Presses de l'Université Laval, Quebec, Canada, 1974), p. 98.

[9]T. Mongan, Phys. Rev. 178, 1597 (1969).

[10]S. Kahana, H. C. Lee, and C. K. Scott, Phys. Rev. 185, 1378 (1969).

[11]F. Tabakin, Ann. Phys. (N. Y.) 30, 51 (1964).

[12]T. F. Hamman and Q. Ho-Kim, Nuovo Cimento 64B, 356 (1969); *ibid.* 67A, 300 (1970).

[13]P. Signell, in *Advances in Nuclear Physics*, edited by M. Baranger and E. Vogt (Plenum, New York, 1969), p. 223.

[14]M. H. MacGregor, R. A. Arndt, and R. M. Wright, Phys. Rev. 182, 1714 (1969).

[15]P. Signell, in *Proceedings of the Symposium on the Two Body Force in Nuclei, Michigan, 1971* (Plenum, New York, 1972), p. 9.

[16]J. Binstock and R. Bryan, Phys. Rev. D 9, 2528 (1974).

[17]H. P. Stapp, T. J. Ypsilantis, and N. Metropolis, Phys. Rev. 105, 302 (1957).

[18]W. Plessas, L. Mathelitsch, F. Pauss, and H. Zingl, Graz report, 1976 (unpublished).

[19]In a separable potential model it is not possible to fit only ϵ_1 without taking $^3S_1$ and $^3D_1$ into consideration.

[20]R. V. Reid Jr., Ann. Phys. (N. Y.) 5, 411 (1968).

[21]R. E. Seamon, K. A. Friedman, G. Breit, R. D. Haracz, J. M. Holt, and A. Prakash, Phys. Rev. 165, 1579 (1969).

[22]N. Hoshizaki, Prog. Theor. Phys. Suppl. 42, 107 (1968).

[23]M. L. Goldberger and K. M. Watson, *Collision Theory* (Wiley, New York, 1964).

[24]J. Blatt and V. Weisskopf, *Theoretical Nuclear Physics* (Wiley, New York, 1952).

[25]F. Pauss, Ph. D. thesis, Univ. of Graz, 1975 (unpublished).

[26]J. E. Simmons, Rev. Nucl. Phys. 39, 542 (1967).

[27]S. W. Johnsen, F. P. Brady, N. S. P. King, M. W. McNaughton, and P. Signell, in *Proceedings of the Fourth International Symposium on Polarization Phenomena in Nuclear Reactions, Zurich, 1975,* edited by W. Grübler and V. König (Birkhäuser Verlag, Basel, 1976), p. 443.

[28]J. P. Scanlon, G. H. Stafford, J. J. Thresher, P. H. Bowen, and A. Langsford, Nucl. Phys. 41, 401 (1963).

[29]L. N. Rothenberg, Phys. Rev. C 1, 1226 (1970).

[30]T. C. Montgomery, F. P. Brady, B. E. Bonner, W. B. Broste, and M. W. McNaughton, Phys. Rev. Lett. 31, 640 (1973).

[31]R. Wilson, *The Nucleon-Nucleon Interaction* (Interscience, New York, 1963), pp. 214, 217.

[32]R. B. Perkins and J. E. Simmons, Phys. Rev. 130, 272 (1963).

[33]A. Langsford, P. H. Bowen, G. C. Cox, G. B. Huxstable, and R. A. J. Riddle, Nucl. Phys. 74, 241 (1965).

[34]R. Hoffmann, J. Lefrancois, E. H. Thorndike, and R. Wilson, Phys. Rev. 125, 973 (1962).